ENGINEERING TRANSACTIONS • *Engng. Trans.* • **55**, 3, 229–238, 2007
Polish Academy of Sciences • Institute of Fundamental Technological Research

EVALUATION OF STEEL CLAD PLATE WELDABILITY USING RAM TENSILE TEST METHOD

Z. Z a t o r s k i

Naval University of Gdynia
Faculty of Mechanical and Electrical Engineering
ul. Śmidowicza 69, 81–103 Gdynia 3, Poland

The weldability evaluation of steel clad plate is performed using the ram tensile test method. Numerical analysis of the considered problem is performed using the finite element method. The author introduces and verifies a critical ram tension strength R_0 above the yield strength R_e^{II} – as the criterion of the weldability evaluation of clad steel plate, where: $R_e^{II}/R_e^I < 0.707$, R_e^{II}, R_e^I – yield strengths of soft and hard materials.

1. Introduction

Cladding may be performed by rolling or explosive welding or by a combination of the two methods. A manufacturer should demonstrate that the required properties of the base material are preserved after cladding [2]. The evaluation of welded connections can be performed by nondestructive methods, for example ultrasonic testing as well as some destructive methods. The destructive methods of the weldability evaluation are introduced by societies of mechanics, especially Requirements of ASTM and GOST. According to them, shear tests and ram tensile tests are performed. Steel-plated sheets are used mainly in the chemical industry, power industry and chemical tankers, where thin contacting plate layers show high corrosion resistance. The next layers of bearing construction are produced from constructional steel. In view of structural inhomogeneity and the similarity of tensile strength of comprised layers, the tearing often runs in weldable zones. It finds also the reflection in the preparation of ram tensile test specimens according to Requirements of ASTM, Fig. 1 [5, 7, 9]. The Requirements of IACS, LRS, GL and PRS prefer the shear test and side bend test [2, 6, 8]. Cracking in weldable zone of clad plate is anticipated in Requirements of ASTM.

The bonding between the base material and clad material should be adequate to ensure that clad material can not separate from the base material when the manufacturing process or service load are applied.

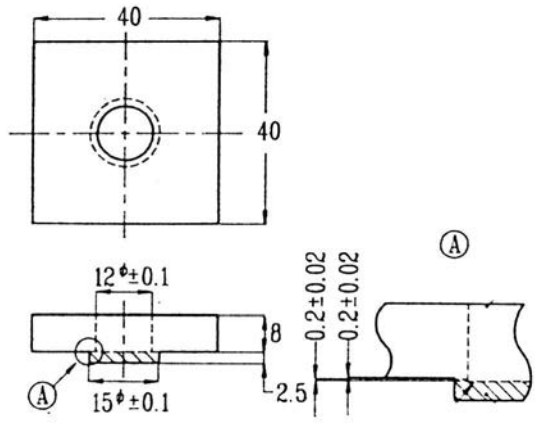

Fig. 1. Dimensions of ram tensile test specimen according to ASTM [5].

The separation processes are localized in the material that has a considerably lower tensile strength. The aim of this paper is elaboration of the ram tensile strength criterion for the above-mentioned clad plates.

2. Experimental procedure

The 30GHMVNb/15G2ANb steel clad plates that have the yield strength $R_{0.2} = 615$ MPa and $R_{0.2} = 325$ MPa, respectively, are supplied inrolled condition for ram tensile tests. The test specimens are cut out in the form of hollow discs. The ram tensile tests are performed on a special test stand as shown in Fig. 2.

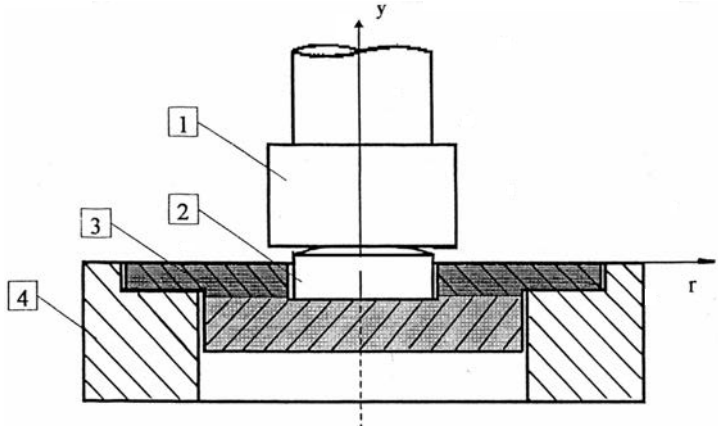

Fig. 2. Test specimen and diagram of the ram tensile test stand, where: 1 – pusher, 2 – stamp, 3 – test specimen, 4 – base.

Characteristic dimensions of the test specimen are shown in Fig. 3.

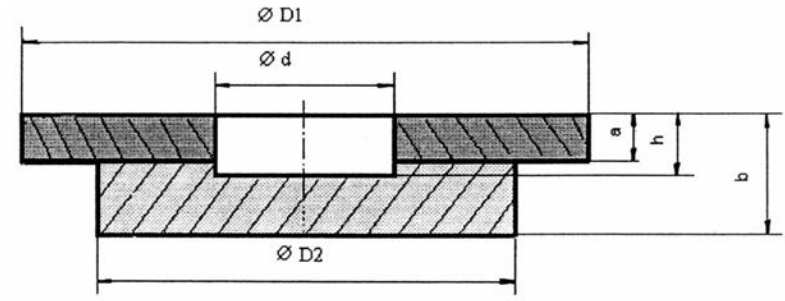

Fig. 3. Characteristic dimensions of the ram tensile test specimen.

The border example of the upper layer is a perfectly rigid material and the bottom layer is a perfectly plastic material. The numerical calculations and experimental verifications will be presented in the following section.

3. Numerical procedures

Experimental observations of the bimaterial system fracture reveal interfacial cracking. The fracture toughness of bimaterial specimen is strongly dependent on the difference in the yield strength and hardening properties of bonded materials. Softening of the material is mainly due to the nucleation and growth processes of microcracks. The coalescence of microcracks leads to the fragmentation process and cracking growth along the interface due to higher stress triaxiality in the softer material. The cracking growth along shear bands in the direction of maximum shear strains reveals away from the interface and into the softer material. From the continuity condition over the interface it follows that when R_e^{II}/R_e^I is less than about 0.7, the harder material remains in the elastic regime [3]. The maximum hoop stress does not occur in harder material just ahead of the crack tip, but away from the interface. The harder phase above the interface constrains the region of plastic deformations and induces high stress triaxiality. Then the maximum mean stress equals

$$\sigma_m = \frac{R_e^{II}}{\sqrt{3}} \left(1 + \frac{3\,\pi}{2}\right), \tag{3.1}$$

if $R_e^{II}/R_e^I < 0.707$, where: R_e^{II}, R_e^I – the yielding stresses of soft and hard materials [3].

Since the voids' nucleation, growth and coalescence result in the growth of damages along the interface, they are under control of mean stresses σ_m and stress triaxiality ξ. Since the maximum shear strains induce the cracking growth

along the shear bands, they are under control of the shear stresses τ and the equivalent stresses σ_H. Both effects should be presented in the numerical analysis of the fracture initiation, especially at geometrical and structural notches of the ram tensile test specimen. The Drucker–Prager flowing condition was adopted by Aifantis [1] and Zhu [10] for metals in view of dependence of the flow stresses K on mean stresses σ_m and expressed by the following equation:

$$f(\sigma_{ij}) = \sqrt{J_2} + \alpha\,\sigma_m - K = 0, \tag{3.2}$$

where: $f(\sigma_{ij})$ – the yielding function, $J_2 = 0.5\ S_{ij} \cdot S_{ij}$ – the second invariant of deviatoric stresses S_{ij}, $S_{ij} = \sigma_{ij} - \sigma_m \cdot \delta_{ij}$, α – the parameter defining the influence of mean stresses $\sigma_m = \sigma_{kk}/3$, $k = 1, 2, 3$ on the flowing stresses K. The ram tensile test method joins the loading force of the test specimen and average stress on the fracture surface. The criterion of average stresses is used to evaluate the clad steel weldability. Finite element method is used to calculate the stresses and strains during simulation of the ram tensile test. The packet of WAT–KAM programmes is applied to calculations. The test specimen is modelled as an axisymmetrical body. The geometry of arrangement with exact qualification of the load and defomation as well as boundary conditions of sub-domains is shown in Fig. 4. The physical model of two-layer steel clad plate is employed for the solution of this problem. Upper layer made of the 30GHMVNb steel and bottom layer of the 15G2ANb steel are used.

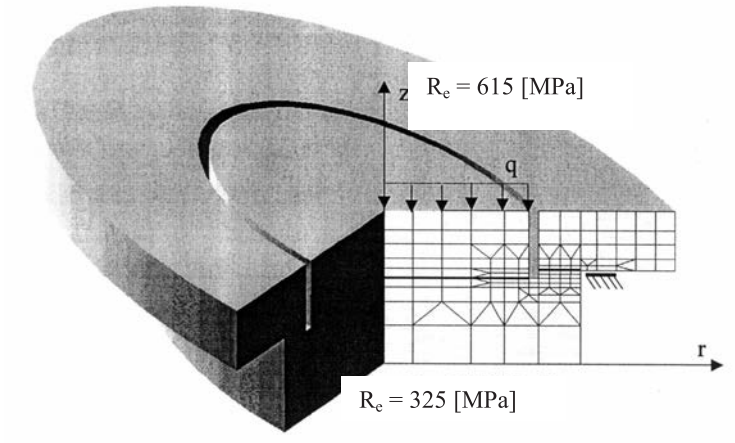

Fig. 4. Geometry of computational arrangement of test specimen for simulation of the ram tensile test.

The stamp is made of the 15G2ANb steel, similarly as the basis. The constant pressure loading is transferred from the pusher to the stamp and then to bottom layer of the test specimen. The support conditions of upper layer of the specimen on the basis are frictionless contact and they are limited to a small surface only.

The boundary conditions determine the global, kinematically admissible displacement field. The boundary conditions on free surface of the specimen

$$\sigma_{ij} \cdot n_j = 0 \qquad (i, j = 1, 2, 3) \tag{3.3}$$

and the continuity conditions on the interface of the specimen are expressed by

$$u_i^{(I)} = u_i^{(II)}, \tag{3.4}$$

$$\sigma_{ij}^{(I)} \cdot n_j = \sigma_{ij}^{(II)} \cdot n_j, \tag{3.5}$$

where: σ_{ij} – Cauchy stress tensor; u_i – displacement coordinate; n_j – coordinate of the unit normal vector with respect to the material interface.

The tensile testing of round – bar tensile specimens is conducted at a constant crosshead velocity, which corresponds to equivalent strain rate $\dot{\varepsilon} = 10^{-3}$ s^{-1} at the room temperature. Physical report to date from static tensile test of the 15G2ANb – EH 32 steel is defined by the hardening law σ_0

$$\sigma_0(\varepsilon_P) = A\,(\varepsilon_0 + \varepsilon_p)^n\,, \tag{3.6}$$

where: σ_0 – yield stress ($\sigma_0(0) = 292$ MPa), A – hardening multiplier ($A = 683.6$ MPa), n – hardening coefficient ($n = 0.1325$), ε_0 – relative elastic deformation ($\varepsilon_0 = 0.00162$), ε_p – relative plastic deformation.

4. Numerical calculations

The results of calculations: equivalent stresses, mean stresses and stress – triaxiality ratios are presented in a graphical form for equivalent stresses σ_H appointed according to the Huber hypothesis. The distributions of equivalent stresses σ_H as well as stress – triaxiality ratios ξ are shown in Figs. 5 – 7 for characteristic specimens thresholds 0.4 mm and 0.2 mm deep. The characteristic values of equivalent stresses σ_H as well as stress – triaxiality ratios ξ are elaborated by means of numerical analysis of ram tensile tests of the 30GHMVNb/15G2ANb steel plate specimens and they are presented in Table 1. The effect of stress – triaxiality ratios distribution ξ on the cracking processes, is especially essential in the ductile cracking analysis in high stress intensity ranges.

Two clear places of crack initiation step out for the test specimen threshold 0.4 mm deep:

- geometrical notch at internal side, and
- structural notch at external side of area of cracking with the continuity of plastic flow.

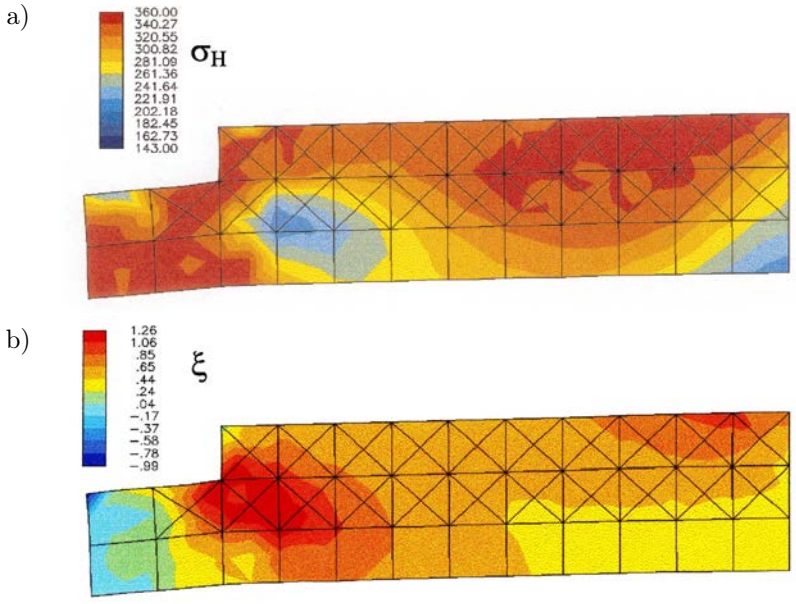

Fig. 5. Equivalent stress distribution σ_H for the 15G2ANb steel layer threshold 0.2 mm deep, of the 30GHMNbV/15G2ANb steel clad plate (a) and stress – triaxiality ratio distribution $\xi = (\sigma_r + \sigma_z + \sigma_t)/3\sigma_H$ (b), for ram tensile test with the load of $F = 38.85$ kN.

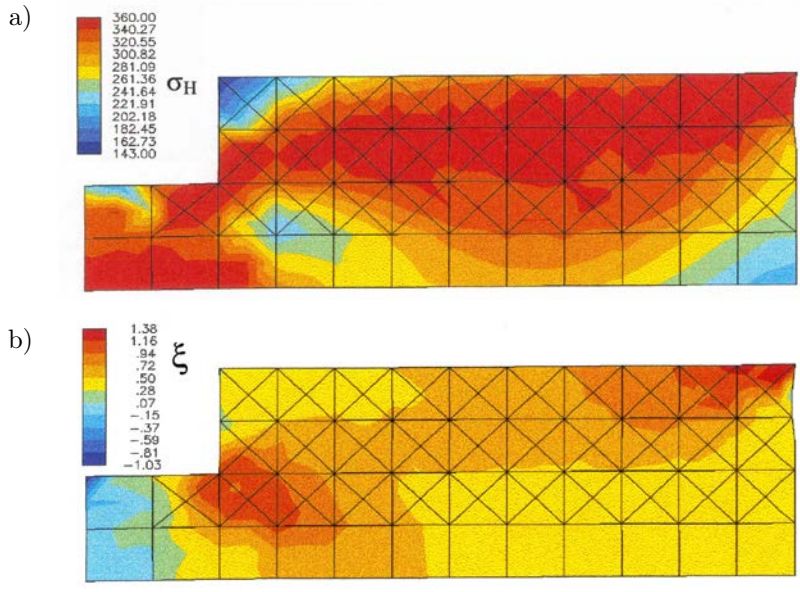

Fig. 6. Equivalent stress distribution σ_H for the 15G2ANb steel layer threshold 0.4 mm deep, of the 30GHMNbV/15G2ANb steel clad plate (a) and stress – triaxiality ratio distribution $\xi = (\sigma_r + \sigma_z + \sigma_t)/3\sigma_H$ (b), for ram tensile test with the load of $F = 38.85$ kN.

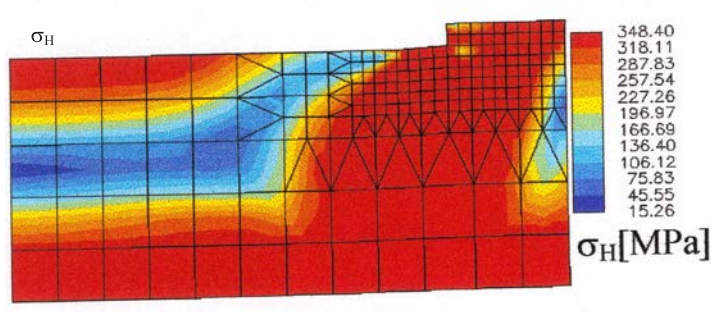

FIG. 7. Equivalent stress distribution σ_H for the 15G2ANb steel layer threshold 0.4mm deep, of the 30GHMNbV/15G2ANb steel clad plate, for ram tensile test with the load of $F = 42.92$ kN.

For the test specimen threshold 0.2 mm deep, the effect of geometrical and structural notches at internal side of cracking area on the stress – triaxiality ratios distribution ξ and equivalent stresses σ_H is clearer with the development of two independent zones of increased plastic flow.

The essential dimensions of the ram tensile test specimen are in approximate agreement with Requirements of the ASTM. It is the reason that good dimensional occuracy of the ram tensile test specimen should be ensured.

The Drucker–Prager flow condition (Eq. (3.2)) is adopted to the following expression

$$K = \sigma_H(1 + \alpha \cdot \xi), \tag{4.1}$$

where $\xi = \sigma_m/\sigma_H$, and the above numerical results are verified according to the experimental data. The highest values of equivalent stresses σ_H as well as stress – triaxiality ratios ξ occur at the specimen threshold 0.4 mm deep as the structural and geometrical notches (1, 3), Table 1.

Table 1. Characteristic values of equivalent stresses σ_H and stress – triaxiality ratios ξ obtained as a result of numerical analysis of ram tensile tests of the 30GHMVNb/15G2ANb steel clade plate.

Designation		Equivalent stress σ_H and stress – triaxiality ratio ξ			
No	specimen threshold	0.2 [mm]		0.4 [mm]	
–	specimen property	σ_H, [MPa]	ξ, [–]	σ_H, [MPa]	ξ, [–]
1	geometr. notch at internal side	340 – 360	1.08 – 1.28	340 – 360	1.10 – 1.30
2	structural notch at internal side	320 – 340	0.24 – 0.44	143 – 162	0.28 – 0.51
3	structural and geometrical notch at external side	320 – 340	0.65 – 0.85	340 – 360	1.10 – 1.30

The load of $F = 42.92$ kN (Fig. 7) produces equivalent stresses σ_H within the range (318–348) MPa with the plastic flow of material in the fracture's area. The highest values of equivalent stresses σ_H occure at the specimen threshold 0.2 mm deep and structural notch at the internal side of specimen (2) at equivalent stresses σ_H within the range (320–340) MPa, Table 1.

5. Experimental Verification

The characteristic dimensions of specimens of the 30GHMVNb/15G2ANb steel clad plate are obtained by means of numerical analysis of the ram tensile tests, Table 2.

The average values of ram tensile strength R_0 are lower than the tensile strength $R_m = 510$ MPa and higher than the yield strength $R_e = 325$ MPa for the 15G2ANb steel of the clad plate.

Table 2. Characteristic dimensions of specimens of the 30GHMVNb/15G2ANb steel clade plate and results of the ram tensile tests.

Designation	Dimensions $D_1 \times D_2 \times d$, [mm]	Maximum load F_0, [kN]	Ram tensile strength R_0, [MPa]
1	$30 \times 20.3 \times 16$	42.5	375
2	$30.1 \times 20.4 \times 16$	41.5	361

The test specimen fracture after the ram tensile test shows effect of the rolled texture and is connected with anisotropy, Fig. 8. The point of crack initiation is placed at geometrical notches of softer layer of clad plate what is confirmed by the numerical calculations.

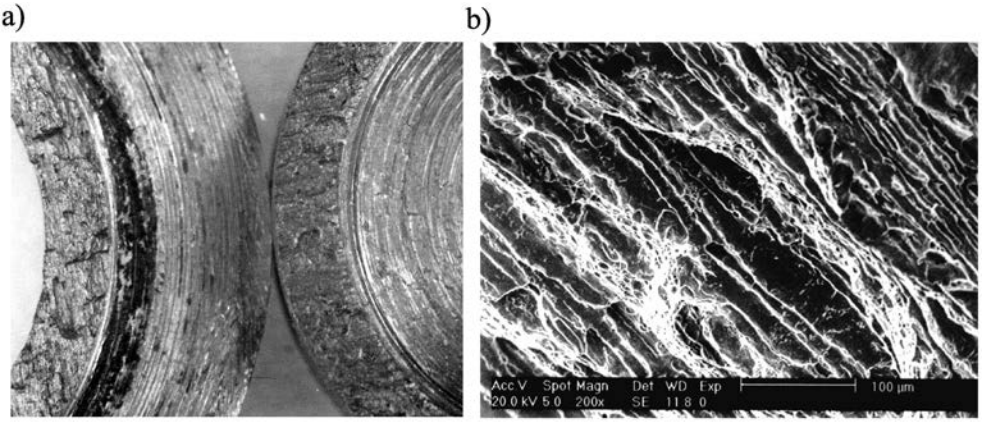

Fig. 8. The ram tensile test specimen fracture (a) and characteristic fracture of the 15G2ANb steel layer of a clad plate, SEM (b).

The plastic flow of material in the fracture area allows to specify possible places of initiation and directions of cracking that has been confirmed by fractographic investigations.

The criterion of weldability evaluation of the clad plate is performed using the ram tensile test. The highest values of equivalent stresses σ_H and stress – triaxiality ratios ξ occur at the the specimen ends as well as at structural and geometrical notches, for the equivalent stresses σ_H above 320 MPa, Table 1. At the same time, the yield strength for the 15G2ANb steel is $R_e = 325$ MPa.

The results presented above show that the plastic flow of soft material is decisive actor in the area of real fracture. On this basis, the author introduces the critical ram tensile strength R_0 higher than the yield strength of soft layer material R_e^{II} as the criterion to evaluate the clad steel plate weldability according to the following inequality

$$R_0 \geq R_e^{II}, \tag{5.1}$$

where $R_e^{II}/R_e^I < 0.707$.

The new criterion differs from the hitherto used, assumed a priori values of critical stresses to evaluate the clad plates weldability according to Requirements of the ASTM.

The parameters of explosive welding conditions can be properly chosen using the ram tensile test and the above criterion [3, 4, 5].

6. Conclusions

1. The criterion to evaluate the clad steel plate weldability is performed using the ram tensile test.
2. The finite element method is used to calculate the stresses and strains during the simulation of the ram tensile test.
3. The author introduces and verifies the critical ram tensile strength R_0, higher than the yield strength of soft layer material R_e^{II}, as a criterion to evaluate the steel clad plate weldability, using the ram tensile test method according to the following inequality

$$R_0 \geq R_e^{II},$$

where: $R_e^{II}/R_e^I < 0.707$, R_e^{II}, R_e^I – the yield strength of soft and hard layer material.

References

1. E.C. Aifantis, International Journal of Plasticity, **3**, 211–217, 1987.
2. Germanischer Lloyd of Shipping, *Rules for classification and construction*, Ch. II, *Material and welding technology*, P.1, Sec.1L, *Clad plates*, 28–30, 1992.

3. S. Hao, W.K. Liu, *Bimaterial interfacial crack growth with strain gradient theory*, Journal of Engineering Materials and Technology, **121**, 10, 413–442, 1999.

4. T. Izuma, K. Hokamoto, M. Fujita, M. Aoyagi, *Single – shot explosive welding of hard – to – weld JIS A5083/SUS304 clad using SUS304 intermediate plate*, Transactions of the Japan Welding Society, **23**, 1, 46–51,1992.

5. K. Hokamoto, T. Izuma, M. Fujita, *New explosive welding technique to weld aluminium alloy and stainless steel plates using a stainless steel intermediate plate*, Metallurgical Transactions A, **24A**, 10, 2289–2297, 1993.

6. Loyd's Register of Shipping, *Rules for the manufacture testing and certification of materials*, P.2., Ch.3, Sec. 7.7, *Clad plates*, 1991.

7. M. Nishida, Z. Murakami, *Behavior of bonded interface of explosive clad steel*, Transactions of the Japan Welding Society, **23**, 1, 9–16, 1992.

8. Polish Register of Shipping, *Rules for Classification and Shipbuilding* [in Polish], 1995, afterwards changes P. IX, Ch.9.5, *Materials and welding, Clad steels,* Gdańsk 1998.

9. W. Walczak, *Explosive welding of metals* [in Polish], WNT, Warszawa 1989.

10. X.H. Zhu, J.E.C. Arsley, W.M. Milligan, E.C. Aifantis, *On the failure of pressure – sensitive plastic materials, Part 1. Models of yield and shear band behavior*, Scripta Materialia, **36**, 6, 721–726, 1997.

Received March 23, 2006; revised version November 2, 2006.